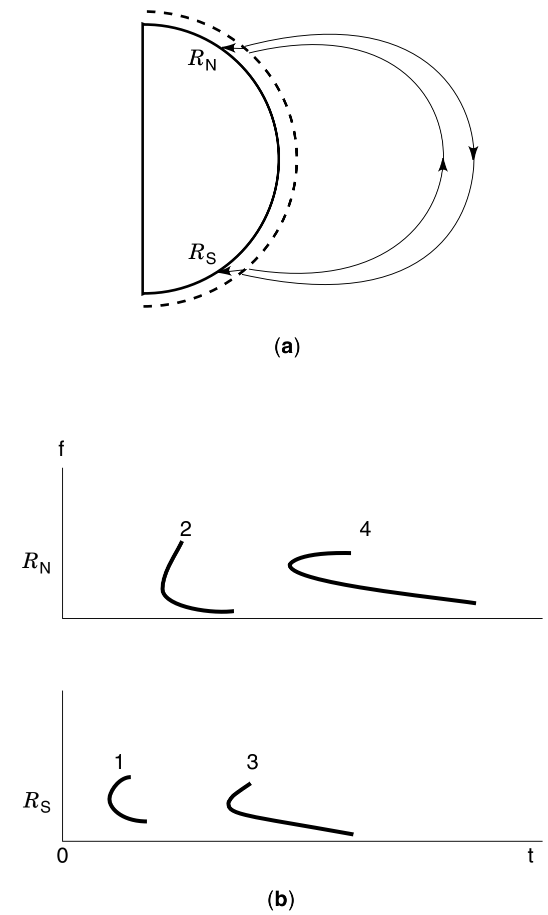

Figure 1. (a) A lightning discharge produces a whistler that echoes from hemisphere to hemisphere along a geomagnetic field line. R_N and R_S are the radio receivers located in the northern and southern hemispheres, respectively. (b) The frequency–time trace of the whistler becomes more elongated with each bounce.

WHISTLERS

Whistlers are bursts of very low frequency (VLF) electromagnetic waves generated by lightning flashes. They are produced when different frequency components of the impulsive lightning pulse travel through the Earth's ionosphere and overlying magnetosphere at different speeds so as to be received usually as a note of decreasing frequency, known as a whistler. The magnetosphere is that near-Earth space, which is on the order of 10 Earth radii in extent, in which the geomagnetic field plays a dominant role in charged particle dynamics. Since whistlers are in the VLF or audio-frequency range (300 Hz to 30 kHz), they can be heard with simple audio equipment, a suitable antenna, an amplifier, and an earphone. The whistling sound is quite distinct, particularly the falling tone, the low-frequency portion of which may last for a second or more. The first unambiguous report of whistlers was made in 1919 by Barkhausen (1). In 1953 Storey (2) showed conclusively that whistlers originated in lightning discharges and gave the correct explanation that whistlers propagated from hemisphere to hemisphere along geomagnetic field lines extending to several earth radii. A fascinating account of the historical background on whistlers is given by Helliwell in his 1965 classic monograph on the subject (3).

THE WHISTLER PHENOMENON

A lightning discharge radiates electromagnetic energy over a wide range of frequencies extending beyond those of visible light. Radiation in a relatively low frequency range, 300 Hz to 30 kHz, is the source of whistlers that propagate through the ionosphere and magnetosphere in the whistler mode. This mode of propagation is possible only in a magnetized plasma at frequencies below both the electron plasma frequency and electron gyrofrequency. Propagation is strongly influenced by the geomagnetic field and is characterized by low propagation speeds that vary with frequency.

If the whistlers are guided through the magnetosphere by field-aligned irregularities, called whistler ducts, they can propagate from hemisphere to hemisphere, as illustrated in Fig. 1. Radiation from a lightning discharge in the northern hemisphere propagates along a duct to the southern hemisphere, and because the different frequency components travel at different speeds, the received signal (one hop whistler) has a frequency–time signature shown by curve 1 with a propagation time delay on the order of 1 s. At the lower edge of the ionosphere in the southern hemisphere, a part of the energy may be reflected back to the northern hemisphere, thus producing a two hop whistler, represented by curve 2. Such partial reflections may repeat many times to produce whistler trains in both hemispheres. When a lightning discharge illuminates more than one duct in the magnetosphere, the resulting whistler consists of several discrete components separated in time due to the differences in travel time through different ducts. Such whistlers are called *multicomponent* or *multipath whistlers.* Many whistlers are preceded by a sharp impulse that sounds like a click when heard through audio amplifier. These impulses called *atmospherics* or *spherics* for short, are produced by lightning discharges that may be thousands of kilometers away. The radiation (spherics) from the lightning discharge travels at approximately the speed of light in the space between the Earth and the lower edge of the ionosphere, called the Earth–ionosphere waveguide. The sound of a distant atmospheric causing a whistler differs very much from that of a nearby whistler source that produces a two-hop whistler in the hemisphere of the observer. The latter type tends to be much more noticeable to an observer and is often characterized by a cluster of impulsive noises or spherics lasting up to several hundred milliseconds. Usually, only one of these spherics is found to be productive of the accompanying whistler. At times when the reflection coefficient of the ionosphere is high, the radiation from a lightning discharge may echo back and forth between the boundaries of the waveguide many times before disappearing into the background noise. Then the received disturbance consists of a series of impulses, which produce a faintly musical or chirping sound associated with the Earth-ionosphere wave-guide cutoff at around 1.6 kHz. This particular type of atmospheric is called a tweek. Figure 2(a) shows an example of a multicomponent whistler observed at Palmer station, Antarctica. The spheric originating from the same lightning discharge that caused the whistler was also detected and is marked by an arrow.

The whistler occurrence rate depends on the local time, season, and location. Whistlers tend to be more common during the night than during the day, mainly because of the relatively high absorption in the daytime ionosphere. They are more frequent at locations and times where lightning storms are common, or at points magnetically conjugate to regions of lightning activity. Whistler occurrence rates are higher in local winter when the thunderstorm activity is high. Whistler activity tends to be greatest at middle latitudes, reaching a maximum in the vicinity of 50° geomagnetic latitude. At the geomagnetic equator, whistlers are virtually unknown; and in polar regions, their rate is significantly lower than in middle latitudes. High occurrence rates for whistlers are observed near the 75° west meridian. This local maximum is apparently associated with the combination of the offset of the geomagnetic and geographic axes and with the high lightning rates in the northern hemisphere along the east coast of the United States and Canada.

With the advent of the Space Age, VLF receivers were placed on many spacecraft and rockets. These spaceborne receivers detected whistlers whose paths deviated significantly from the Earth's magnetic field lines. Such whistlers, called *unducted or nonducted* whistlers, show a wide variety of frequency–time signatures, depending on the location of the receiver (spacecraft) with respect to the causative lightning discharge, and on the density distribution of electrons and ions in the magnetosphere. By the nature of their propagation mode, these unducted whistlers cannot be detected on ground. Figure 2(b) shows an example of a whistler observed on the Dynamic Explorer 1 (DE 1) satellite. The spacecraft observations of unducted whistlers have led to a new understanding of many subtle features of whistler-mode propagation and to the deduction of important plasma parameters in space. Spacecraft-borne VLF receivers also detected new kinds of whistlers, called *ion whistlers* (in contrast to conventional electron whistlers). Ion whistlers, not seen on the ground, occur at much lower frequencies, ~100 Hz to 500 Hz and are related to the effects of ions.

When whistlers were explained as radiation from lightning that had traveled several earth radii out into space, it became clear that they contained useful information about the medium through which they propagated. Methods were developed to infer plasma density in the magnetosphere. This led to the discovery of the *plasmapause,* an important boundary in the inner magnetosphere where the equatorial electron density drops abruptly by a factor of 10 to 100. Whistlers also provided a means of measuring electric fields in the magnetosphere and the flow of plasma between the magnetosphere and the ionosphere.

Whistlers interact with energetic electrons in the radiation belts during their traversal through the magnetosphere. Such interactions may result in the amplification of the whistlers, triggering of emissions at new frequencies, and precipitation of some of the interacting energetic electrons in the radiation

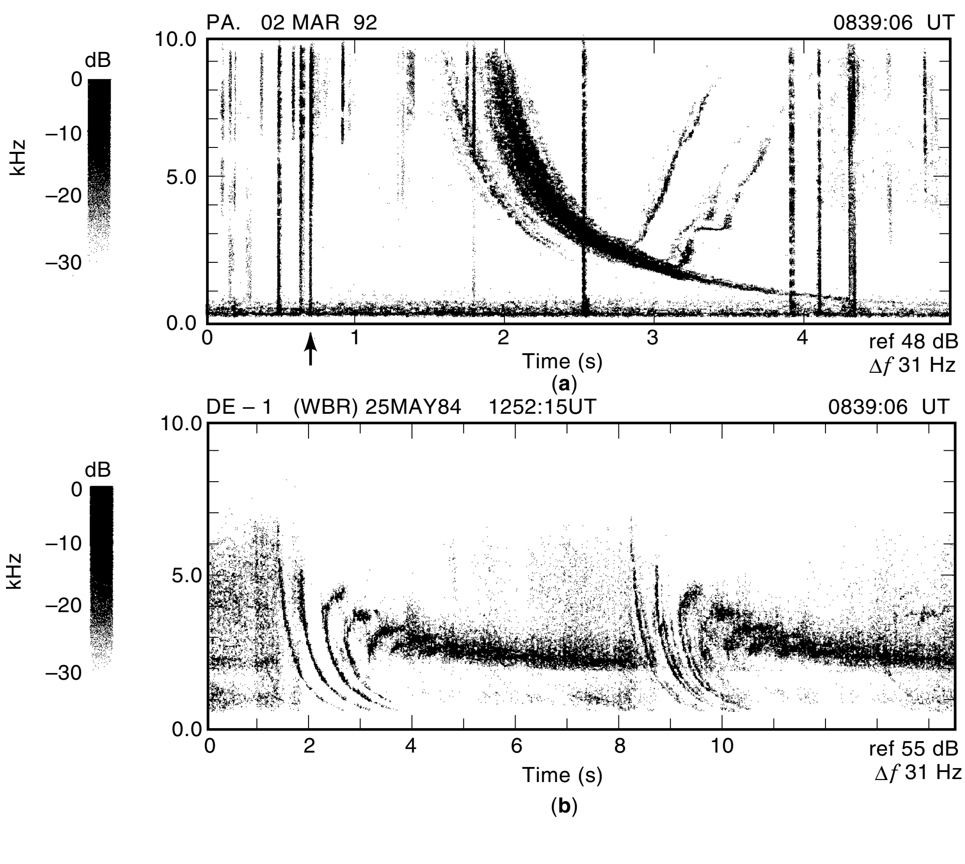

Figure 2. (a) Spectrogram of a multicomponent ducted whistler received at Palmer Station, Antarctica, and the associated triggered emissions. (b) Spectrogram of nonducted MR whistlers observed on the high altitude polar orbiting DE 1 satellite. (Courtesy of VLF group, Stanford University.)

belts. Precipitating electrons, in turn, produce enhanced ionization and optical emissions in the lower ionosphere, as well as X rays detectable down to about a 30 km altitude. Whistlers generate *lower hybrid waves* that can accelerate ions to suprathermal energies. It has also been suggested that whistlers contribute to the generation of plasmaspheric hiss, which is believed to be responsible for the dynamic equilibrium of the radiation belts and for the presence of the slot region in the radiation belt.

Related to whistler phenomenon are other ionospheric and magnetospheric waves which propagate in the whistler mode but originate either in magnetospheric sources or in the humanmade sources such as VLF transmitters. These naturally occurring waves, also occurring in the VLF band and collectively called VLF emissions, have been labeled as hiss, chorus, and lion's roar, based on the aural sound they produce when heard through audio amplifiers. Unlike whistlers, the generation mechanisms of these other wave phenomena are poorly understood, and they remain the focus of intense research activity.

In the following sections we briefly discuss the history of whistlers, theoretical background, observations, and the effects of whistlers on the Earth's geospace. For a more detailed treatment of whistlers we refer readers to the classic monograph by Helliwell (3), and review papers by Park (4) and Hayakawa (5), and for a recent review of whistler-mode VLF emissions other than lightning-generated whistlers we refer to a review by Sonwalkar (6).

WAVE PROPAGATION IN A COLD MAGNETOPLASMA

The salient features of the whistlers received on the ground can be explained by the classical magneto-ionic theory found in detail in several textbooks such as Budden (7), Stix (8). This theory takes into account the motion of electrons but ignores their thermal motion as well as the motion of ions. The ion effects are important for waves propagating at large wave normal angles with respect to the geomagnetic field and thus important for nonducted whistlers observed on satellites. The effects of ion motion on wave propagation will be discussed in a later section on unducted propagation. Collisions between electrons and heavy particles are important in the D-region (90 km) of the ionosphere and lead to significant absorption of waves, but have negligible effects on propagation of whistlers throughout most of the magnetosphere above the D-region. In the following discussion we shall neglect the collisional effects, and treat them separately in the section on ionospheric propagation.

Appleton–Hartree Equations

Figure 3 shows the geometry describing the propagation of a plane wave in the z-direction at an angle θ, called the wave normal angle, to the static (geomagnetic) magnetic field $\boldsymbol{B}_0$. The electric field $\boldsymbol{E}(z, t)$ of this plane wave of frequency f is given by

$$\boldsymbol{E}(z,t) = \mathrm{Re}[(E_x\boldsymbol{x} + E_y\boldsymbol{y} + E_z\boldsymbol{z})\exp\{i(\omega t - kz)\}] \qquad (1)$$

where E_x, E_y, and E_z are the phasor components of electric field of the wave, $i = \sqrt{-1}$, $\omega = 2\pi f$ = wave angular frequency, k = wave number, and t represents time. Re stands for the real part of the expression in brackets.

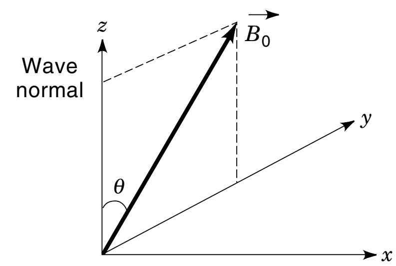

Figure 3. The coordinate system showing the wave normal direction and the geomagnetic field direction.

It is convenient to define wave refractive index n as the ratio of the velocity of light in free space $c = 3 \times 10^8$ m/s and the phase velocity $v_p = \omega/k$ of the wave.

$$n = \frac{c}{v_p} = \frac{ck}{\omega} \qquad (2)$$

The relation between k and ω defined by Eq. (2) is called the *dispersion relation.* The vector quantity $\boldsymbol{k} = k\boldsymbol{z}$ is called the wave normal vector, and for a given frequency, $\boldsymbol{k}$ includes information about both the direction of propagation and the phase velocity of the wave.

The wave magnetic field $\boldsymbol{H}$ is given from Maxwell's equations in terms of the wave electric field.

$$\boldsymbol{H}(z,t) = \frac{\boldsymbol{k}\times\boldsymbol{E}}{\mu_0\omega} \qquad (3)$$

where $\mu_0 = 4\pi \times 10^{-7}$ H/m is the free space permeability.

The Appleton–Hartree equations represent solutions to Maxwell's equations for wave propagation in a uniform, homogenous magnetoplasma. The solutions are given in terms of the expressions for wave refractive index n, and the wave polarization $p = E_x/E_y$ and $s = E_z/E_x$ as a function of wave frequency, wave normal angle, and the medium parameters.

$$n^2 = 1 - \frac{X}{1 - \dfrac{1/2Y_T^2}{1-X} \pm \dfrac{1}{1-X}[1/4Y_T^4 + Y_L^2(1-X)^2]^{1/2}} \qquad (4)$$

$$\begin{aligned} p &= \frac{E_x}{E_y} = -\frac{H_y}{H_x} \\ &= -\frac{i}{Y_L(1-X)}\{1/2Y_T^2 \mp [1/4Y_T^4 + Y_L^2(1-X)^2]^{1/2}\} \end{aligned} \qquad (5)$$

$$s = iY_T\frac{n^2-1}{1-X}E_x \qquad (6)$$

Where $X = f_p^2/f^2$; f_p = electron plasma frequency = $1/2\pi(Ne^2/\epsilon_0 m_e)^{1/2}$; N = electron concentration; e = electron charge = 1.6021×10^{-19} C; ϵ_0 = dielectric constant of free space = 8.854×10^{-12} F/m; m_e = electron mass = 9.1066×10^{-31} kg; $Y = f_H/f$; f_H = electron gyrofrequency = $1/2\pi(B_0 e/m_e)$; $Y_T = Y \sin\theta$; and $Y_L = Y\cos\theta$.

These equations are known as the Appleton–Hartree equations. Depending on the values of X and Y, that is, values of plasma and gyrofrequency relative to the wave frequency, Eq.

(4) represents many different modes of propagation. Each mode is specified by a characteristic refractive index n (or phase velocity v_p, and the polarizations p and s. Various schemes are used to label various modes (7,8), depending on the nature of the refractive index of waves propagating parallel or perpendicular to $\boldsymbol{B}_0$ and/or the polarization of waves.

As the wave propagates it may encounter regions where the values of the plasma parameters are such that the refractive index n goes to zero, a *cutoff,* or infinity, a *resonance.* In going through a cutoff n goes through zero, and the transition is made from a region of possible propagation to a region of evanescence. Generally, a reflection occurs in this circumstance. Resonance occurs for propagation at certain frequencies and at certain wave normal directions. In the transition region between propagation and evanescence which occurs when n goes through ∞, absorption or reflection may occur. The frequency at which cutoff occurs for a given mode is called the cutoff frequency of that mode. The frequency and angle at which resonance occurs for a given mode are called resonance frequency and resonance cone angle, respectively.

The Whistler Mode

The whistler mode is named after the lightning-generated whistlers which propagate in this mode (3). The whistler mode propagates at frequencies below either the plasma frequency, f_p, or the gyrofrequency, f_H, whichever is lower. The whistler mode corresponds to the choice of the negative signs in Eqs. (4) and (5). The whistler mode is characterized by large values of refractive index or slow propagation speeds. At $\theta = 0$ the polarization is right hand circular (R) so that the wave field vectors rotate around $\boldsymbol{B}_0$ in the same sense as electrons do in their gyromotion. Waves propagating in this mode are found throughout the magnetosphere (6).

For $\theta = 0$, resonance ($n \to \infty$, $v_p \to 0$) occurs either at $X = 1$ or $Y = 1$, limiting the region of propagation to $X > 1$ and $Y > 1$: that is, wave frequency, f, less than both the plasma frequency and gyrofrequency. For $\theta \neq 0$, the resonance is given by

$$Y = \left(\frac{X-1}{X\cos^2\theta - 1}\right)^{1/2} \tag{7}$$

Refractive Index Surface. It is clear from Eq. (4) that a magnetoplasma is an anisotropic (n depends on θ) and dispersive (n depends on f) medium. Figure 4 shows a polar plot of n versus θ for three different values of Y. Since there is an azimuthal symmetry around $\boldsymbol{B}_0$, the refractive index surfaces are generated by the revolution of $n - \theta$ curves around $\boldsymbol{B}_0$. The

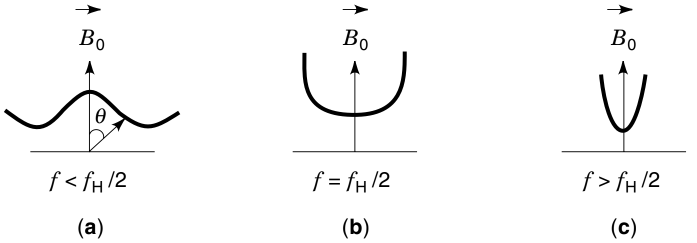

Figure 4. The refractive index as a function of wave normal direction for (a) $f < f_H/2$, (b) $f = f_H/2$, and (c) $f > f_H/2$.

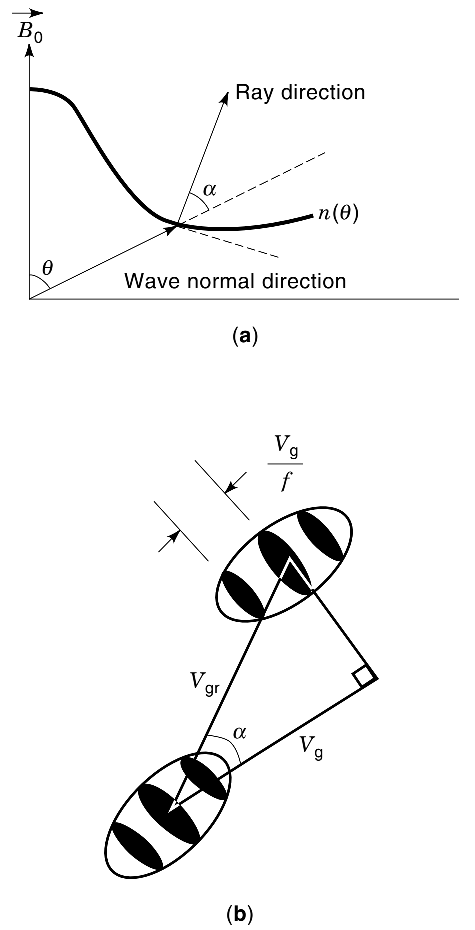

Figure 5. (a) The relationship between wave normal direction and ray direction. (b) Schematic illustration of phase velocity, group velocity, and group ray velocity.

angle at which $n \to \infty$ is called the resonance angle, θ_R, and it lies on a cone called the resonance cone. Equation (7) gives

$$\theta_R = \cos^{-1}\left(\frac{X + Y^2 - 1}{XY^2}\right)^{1/2} \tag{8}$$

Ray Direction, Ray Group Velocity and Ray Refractive Index. In an anisotropic medium, a wave packet travels in a direction different from the wave normal direction. The direction of the wave packet is the direction of propagation of energy and is called the ray direction. It can be shown (1) that the ray direction is normal to the refractive index surface as illustrated in Fig. 5(a). The angle α between the ray direction and wave normal angle is given by

$$\tan\alpha = -\frac{1}{n}\frac{\partial n}{\partial \theta} \tag{9}$$

At low frequencies, as can be seen from Fig. 5(a), the ray direction does not depart much from the static magnetic field and in the zero frequency limit can be shown to be limited to $\sim$19.3° with respect to the direction of $\boldsymbol{B}_0$ (2). Thus, the anisotropy provides a certain amount of guiding of the energy along the geomagnetic field. The group velocity of a wave packet is defined as $v_g = \partial\omega/\partial k$ in the direction of the wave normal, and the group refractive index as $n_g = c/v_g$, which is related to the refractive index by

$$n_g = \frac{\partial}{\partial f}(nf) \tag{10}$$

Since in an anisotropic medium, the ray direction is different from the wave normal direction, the actual ray velocity or group ray velocity v_{gr} is given by

$$v_{gr} = \frac{v_g}{\cos\alpha} = \frac{c}{n_{gr}} = \frac{c}{n_g \cos\alpha} \tag{11}$$

where n_{gr} is the group refractive index. Figure 5(b) shows the relationship between the phase, group, and group ray velocities.

Quasi-Longitudinal Approximation. Equations (4) and (5) are difficult to use because of their complexity. However, for relatively small wave normal angles, considerable simplification is possible by ignoring terms involving Y_T. The propagation is called longitudinal for $\theta = 0$ and quasi-longitudinal (QL) for small values of θ. Specifically, if the condition

$$\frac{\sin^2\theta}{\cos\theta} < \frac{2}{3}\frac{f_p^2}{ff_H} \tag{12}$$

is satisfied, we can approximate the Eqs. (4) and (5) by

$$n^2 = 1 - \frac{X}{1-|Y_L|} = 1 + \frac{f_p^2}{ff_H\cos\theta - f^2} \simeq \frac{f_p^2}{ff_H\cos\theta - f^2} \tag{13}$$

$$p = -i\,\frac{|Y_L|}{Y_L} \tag{14}$$

In these equations the negative in Eqs. (4) and (5) has been retained to represent the whistler mode. The quantity Y_L is either positive or negative, depending on the value of θ (note that the sign of Y is negative for electrons).

Using Eq. (13) in Eq. (10) we obtain the group refractive index

$$n_g = \frac{1}{2}\frac{f_p f_H \cos\theta}{f^{1/2}(f_H\cos\theta - f)^{3/2}} \tag{15}$$

Since the quantity f_p^2/ff_H is usually much larger than unity, the QL approximation is valid up to large values of θ.

PROPAGATION THROUGH THE IONOSPHERE

The typical free-space wavelength at whistler frequencies of 1 kHz to 30 kHz range from 300 km to 10 km. Since in the lower ionosphere (~60 km to ~500 km altitude) refractive index varies rapidly with vertical distances less than a wavelength, the usual assumption that the medium is slowly varying is not valid in the ionosphere. Under these circumstances waves undergo partial reflections and mode coupling whose analysis requires full wave solutions. However, certain aspects of whistler propagation through the ionosphere can be examined with the help of a few basic principles.

Snell's Law and the Transmission Cone

Consider a wave propagating across the boundary between two horizontally stratified media with different refractive indices n_1 and n_2, as illustrated in Fig. 6(a). *Snell's law* states

$$n_1 \sin\delta_1 = n_2 \sin\delta_2 \tag{16}$$

where δ_1 and δ_2 are the angles that the wave normal makes with the normal to the interface in medium 1 and 2, respectively. This law is also applicable to anisotropic media. Consider the air–ionosphere boundary at the lower edge of the ionosphere, as shown in Fig. 6(b). For the propagation in the ionosphere, the refractive index depends on the wave normal angle θ. Therefore, Snell's law can now be written as

$$n_1 \sin\delta_1 = n_2(\theta) \sin\delta_2 \tag{17}$$

For a wave incident on the ionosphere from below, $n_1 = 1$. Since the whistler mode refractive index in the ionosphere is large compared to unity, all waves that enter the ionosphere from below with different wave normal angles have their wave normal angles bent sharply toward the vertical so that they lie within the shaded region, called the transmission cone. For example, at the ionospheric F-layer where the electron density is ~10^6, n_2 is of the order of 100 for a wave frequency of 5 kHz. This gives a very narrow transmission cone with maximum allowed δ_2 of ~0.5°. Thus, we conclude that

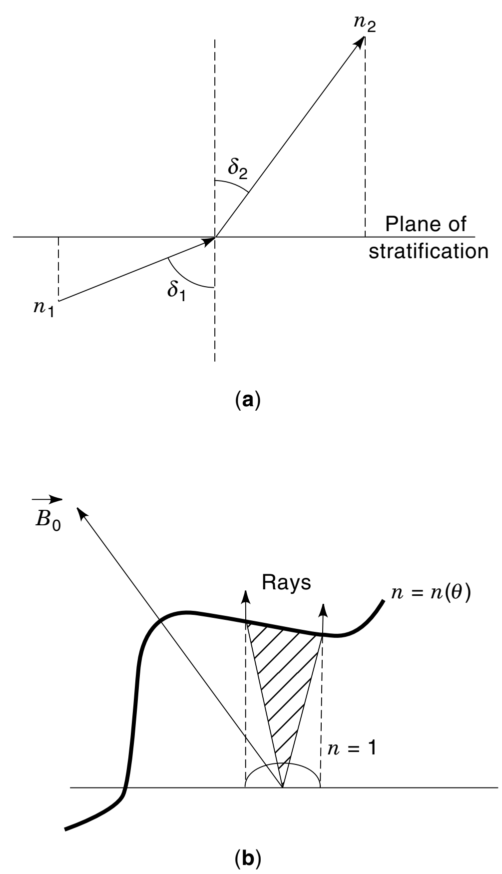

Figure 6. (a) An illustration of Snell's law at a boundary between two media with different refractive indices. (b) An illustration of the transmission cone at the lower boundary of the ionosphere.

any whistler mode wave originating in the atmosphere (e.g., lightning) enters the magnetosphere with an essentially vertical wave normal angle.

After a whistler wave propagates through the magnetosphere and reaches the conjugate ionosphere, the reverse problem exists. If the wave normal angle of the wave incident from above is inside the transmission cone, it can propagate through the ionosphere into the Earth–ionosphere wave guide. If it is outside the transmission cone, the wave will be reflected back into the magnetosphere. Such reflection is called total internal reflection.

Ionospheric Absorption

Electron collisions with neutral air molecules in the lower ionosphere result in the loss of wave energy. Effects of collisions lead to a complex refractive index, its imaginary part being the attenuation factor. In the QL approximation, with some simplifying assumptions, it can be shown (3) that the attenuation constant γ in nepers per meter is given by

$$\gamma = \frac{f_p \nu f^{1/2}}{2c/f_H \cos\theta|^{3/2}} \quad (18)$$

where ν is the collision frequency.

Equation (18) shows that the absorption increases with frequency. Calculations with a model ionosphere show that γ has a sharp peak at about 80 km altitude (D-region of the ionosphere). The total ionospheric absorption of whistler waves can be estimated by integrating Eq. (18). A consequence of D-region absorption is that many magnetospheric wave phenomena are better observed at night time when the D-region absorption is minimum, and about 10 dB less than that in daytime (3).

PROPAGATION THROUGH THE MAGNETOSPHERE

Whistler propagation in the magnetosphere takes place in two different ways: One way is ducted propagation, in which the whistler propagates along field-aligned plasma density irregularities called ducts (9). These whistlers are observed on the ground and are called ducted whistlers. The second way is unducted propagation, in which whistlers are guided primarily by the geomagnetic field and large-scale density gradients in the magnetosphere (10). These whistlers, called unducted or nonducted whistlers undergo multiple reflections within the magnetosphere and never reach the ground. Consequently, they are observed only on spacecraft.

Ducted Propagation in the Magnetosphere

As discussed in the section on Snell's law, whistlers emerging from the magnetosphere must have their wave normal angles within a narrow transmission cone around the vertical in order to propagate through the ionosphere and be observed on the ground. Waves with wave normal directions outside the transmission cone are reflected back into the ionosphere. Furthermore, if the downcoming wave normal directions deviate significantly from the geomagnetic field in the topside ionosphere, the wave is reflected back into the magnetosphere by the lower hybrid resonance (LHR) reflection mechanism discussed in the next section on nonducted propagation. Although the anisotropy of the medium provides some guiding of whistler waves in the magnetosphere, in general this guiding alone is insufficient to prevent LHR reflection. Additional guiding by field-aligned plasma density irregularities, called ducts, is required for ground-to-ground whistler propagation. Figures 7(a) and 7(b) shows typical ray paths for ducted and nonducted propagation, respectively.

Because the refractive index surface goes through a topological change (see Fig. 4) at $f/f_H = \frac{1}{2}$, conditions for ducting also change at that frequency. The Snell's construction shows that the density gradients on both sides of a crest tend to rotate the wave normal toward the geomagnetic field direction. For frequencies below $f_H/2$, the refractive index surface is concave downward. This geometry requires a density crest for ducting. For frequencies above $f_H/2$, the refractive index surface is concave upward. This geometry requires a density trough for ducting. However, since this mode of ducting requires $f > f_H/2$, the wave frequency must be ~0.5 MHz or higher in order to be ducted all the way down to the ionosphere. Thus, this type of ducting does not apply to whistlers. We conclude that whistlers received on the ground require enhancement ducts and that ducting should be effective up to one half of the minimum electron gyrofrequency along the path. Alternatively, a ducted whistler propagating along a certain geomagnetic field line will show an upper cutoff at half the gyrofrequency at a point where the field line crosses the equator. Both ground and spacecraft observations of whistlers confirm this upper frequency cutoff (11). It can be shown that ducts need not have density gradients on both sides to guide the waves from hemisphere to hemisphere. Thus, the plasmapause, where the density decreases sharply with increasing radial distance, provides an excellent one-sided whistler duct (12).

How ducts are formed is not well understood, but whistler observations suggest that they are prevalent throughtout the middle magnetosphere ($L \simeq 2$ to 6) under normal geomagnetic conditions. The parameter L is used to describe a specific magnetic shell or a magnetic field line. For example, an $L = 4$ magnetic field line crosses the geomagnetic equator at a geocentric distance of $4R_E$ in a dipole field. The probability of duct occurrence decreases below $L \simeq 2$ and beyond the plasmapause. The lifetime of a duct varies from a few minutes to many hours. There are few measurements of ducts made on spacecraft (13,14). These indicate that typical duct widths are of the order of 0.1 L, enhancement of 25%, and longitudinal width of about 4°.

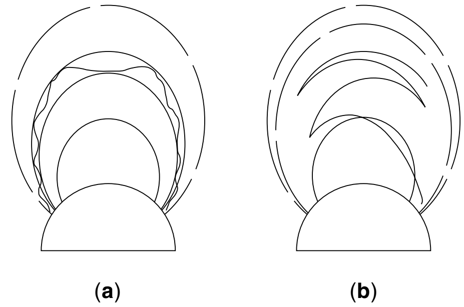

Figure 7. An illustration of different ray paths for (a) ducted and (b) nonducted whistler-mode propagation in the magnetosphere.

Time Delay and Dispersion. For ducted whistlers propagating from hemisphere to hemisphere, we may assume that both the wave normal and ray direction are always parallel to the geomagnetic field ($\theta = 0$, $\alpha = 0$). With these assumptions, we obtain from Eqs. (13) and (15) the following expression for the whistler travel time as a function of frequency.

$$T(f) = \int_{\text{path}} \frac{ds}{v_g} = \frac{1}{c}\int_{\text{path}} n_g\, ds = \frac{1}{2c}\int_{\text{path}} \frac{f_p}{f^{1/2} f_H^{1/2}\left(1 - \dfrac{f}{f_H}\right)^{3/2}}\, ds \qquad (19)$$

If f_p and f_H are specified as a function of distance along a magnetic field line, the integral in Eq. (25) can be numerically integrated to obtain the whistler travel time as a function of frequency. For realistic magnetospheric models, $T(f)$ has a minimum, t_n, at a frequency, f_n, as illustrated in Fig. 8. Whistlers exhibiting a minimum time delay on a spectrogram are called nose whistlers, f_n is the nose frequency, and t_n is the nose delay (15). These parameters, f_n and t_n, are related to the path location or the L value of the duct and the electron density along the path.

At low frequencies such that $f \ll f_H$ along the entire propagation path, Eq. (19) can be approximated by

$$T(f) = \frac{1}{c}\int_{\text{path}} n_g\, ds = \frac{1}{2c}\int_{\text{path}} \frac{f_p}{f^{1/2} f_H^{1/2}}\, ds \qquad (20)$$

From Eq. (20) we see that it is possible to define a parameter D, called dispersion, given by

$$D \equiv t f^{1/2} = \frac{1}{c}\int_{\text{path}} n_g\, ds = \frac{1}{2c}\int_{\text{path}} \frac{f_p}{f_H^{1/2}}\, ds \qquad (21)$$

which is independent of the wave frequency. This approximation, valid at frequencies much below the nose frequency, is known as the Eckersley dispersion law (3).

Remote Sensing of the Magnetosphere From Ground-Based Whistler Observations. Powerful techniques have been developed to determine the magnetospheric electron densities from the observed time delays $T(f)$ of ducted whistlers. These methods generally assume a diffusive equilibrium model for the magnetosphere inside the plasmasphere where plasma densities are of the order of ~100 per cm^3 and a collisionless power law model of R^{-N} for the region beyond the plasmapause where plasma densities are of a few electrons per cubic centimeter. The measured $T(f)$ is then used to estimate the model parameters (4). The plasmapause, first discovered by the whistler technique, is a permanent feature of the magnetosphere that results from a large-scale convection of the magnetospheric plasma driven by the solar wind. Whistler rates vary greatly with location, season, geomagnetic activity, and other factors, but in certain areas such as Western Antarctica, the rates are usually sufficiently high to allow routine measurement of electron density profiles.

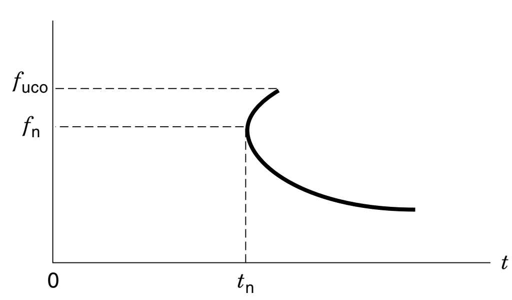

Figure 8. A nose whistler with a sharp upper cutoff.

Another application of the whistler technique is the measurement of plasma drift velocity and the large-scale electric fields in the magnetosphere. If a whistle duct drifts radially inward (outward), the nose frequency increases (decreases) with time. By measuring f_n for successively recorded whistlers, we can obtain the changes with time of the L-shell of the duct along which a whistler propagates. The drift velocity $\boldsymbol{v}_d$ is caused by an electric field, and is given by (4)

$$\boldsymbol{v}_d = \frac{\boldsymbol{E} \times \boldsymbol{B}_0}{B_0^2} \qquad (22)$$

Assuming a dipole model for $\boldsymbol{B}_0$, we can show (4)

$$E_W = 2.1 \times 10^{-2} \frac{df_n^{2/3}}{dt} V/m \qquad (23)$$

where E_W is the east–west component of the electric field. If df_n/dt is positive (inward drift of the duct), then the electric field is oriented east–west. Electric field as small as 10^{-5} V/m can be measured by this technique (16). Sazhin, Hayakawa, and Bullough (17) have reviewed the whistler techniques to measure various magnetospheric parameters and the main results obtained by the application of these techniques.

Nonducted Propagation in the Magnetosphere

In the nonducted or unducted mode of propagation, both the wave normal and ray path deviate significantly from the geomagnetic field direction. Therefore, one cannot use the QL approximation used for the ducted propagation. The calculation of ray paths requires use of the full expression for refractive index and computational ray tracing method in a model magnetosphere. Furthermore, at large wave normal angles, the motion of ions strongly influence the propagation and must be included in the analysis of propagation paths (7,8).

Effect of Ions. The magnetospheric plasma is composed of electrons and ions of a few species including hydrogen (proton), helium, and oxygen. The effect of including ions is to modify the expressions for refractive index and polarization (10–12), add new zeros and resonances, and thus provide additional modes of propagation.

As an example, the refractive index for longitudinal ($\theta = 0$) propagation with one ion species included is given by

$$n^2 = 1 - \frac{X_e}{1 \pm Y_e} - \frac{X_i}{1 \mp Y_i} = 1 - \frac{f_{pe}^2 + f_{pi}^2}{(f \pm f_{He})(f \mp f_{Hi})} \qquad (24)$$

where the subscripts e and i denote electron and ion, respectively, and all quantities are defined in a manner analogous to those in Eq. (4). Since the ion mass is much larger than electron mass, $|X_e| \gg |X_i|$ and $|Y_e| \gg |Y_i|$, and ion effects become significant at lower frequencies.

For transverse ($\theta = 90°$) propagation, the effect of ions is to modify the refractive index such that two new resonance ($n \to \infty$) frequencies, $f_{\rm LHR}$ and $f_{\rm UHR}$ appear. These are called lower hybrid resonance (LHR) and upper hybrid resonance (UHR), respectively. With the condition $f_{pe} \gg f_{He} \gg f_{Hi}$, usually satisfied in the ionosphere and magnetosphere, the expression for $f_{\rm LHR}$ is given by

$$\frac{1}{f_{\rm LHR}^2} = \frac{1}{f_{He}f_{Hi} + \dfrac{f_{He}}{f_{Hi}f_{pe}^2}} \tag{25}$$

For a dense plasma, the expression for $f_{\rm LHR}$ is further simplified.

$$f_{\rm LHR} = \sqrt{f_{He}f_{Hi}} \tag{26}$$

Satellite observations frequently show a strong LHR noise stimulated by whistlers or generated spontaneously by plasma instability (18). Such noise shows a sharp low-frequency cutoff at the local $f_{\rm LHR}$. Measured $f_{\rm LHR}$ can be used to determine f_{pe} if f_{He} and m_i are known, or to determine m_i, if f_{pe} and f_{He} are known (19,20).

With the similar approximation, the expression for $f_{\rm UHR}$ is

$$f_{\rm UHR} = (f_{pe}^2 + f_{He}^2)^{1/2} \tag{27}$$

The upper hybrid resonance frequency lies outside the whistler mode frequency range and has no effect on whistler propagation. Satellite observations of $f_{\rm UHR}$ have proven useful in measuring plasma densities in the magnetosphere (4).

The lower hybrid resonance profoundly affects the propagation of nonducted whistler mode propagation. The most notable feature of the ion effect on whistler mode propagation is that it allows transverse propagation for frequencies below $f_{\rm LHR}$. Figure 9 shows the refractive index as a function of θ with and without ion effects. The frequency is assumed to be below $f_{\rm LHR}$. Without ions, the refractive index goes to infinity at the resonance angle θ_R given by Eq. (8), and propagation is not possible for wave normal angles greater than the resonance angle. If ion effects are included, the refractive index curve becomes closed, and propagation is possible for all wave normal angles (21). Above the LHR frequency, the refractive index does not close even when ions are included, and propagation is not possible for angles larger than resonance angle.

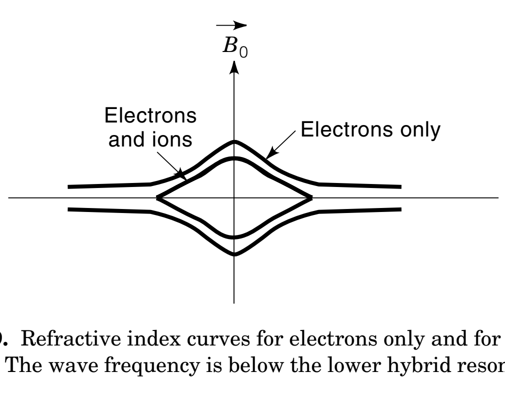

Figure 9. Refractive index curves for electrons only and for electrons and ions. The wave frequency is below the lower hybrid resonance frequency.

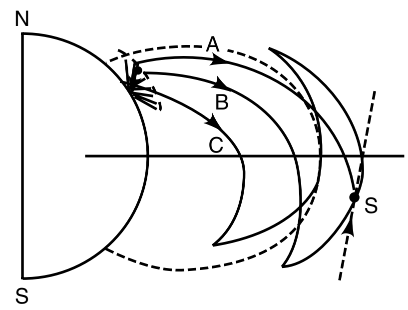

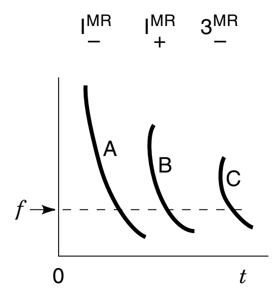

Figure 10. Three different unducted propagation paths from a lightning source to a satellite are shown at left (a) for a given frequency. The paths vary with frequency, and the resulting frequency–time behavior of received signals is as shown at right (b). Each discrete trace is designated by the number of hops N and a subscript, + or −. If the last incomplete hop crosses the equator, the trace is designated by $(N + 1)_-$. If it does not cross the equator, it is designated by N_+ (From R. L. Smith and J. J. Angerami, *J. Geophys. Res.,* **66**: 3699, 1968. Copyrighted by the American Geophysical Union. With permission.)

Magnetospherically Reflected Whistlers. The initial wave normal angle of a whistler entering the ionosphere is nearly vertical. Spatial gradients in the refractive index tend to rotate the wave normal toward the magnetic field direction but not as rapidly as the field direction itself rotates. Consequently, the wave normal angle increases steadily toward the resonance cone angle. As the ray travels past the equator and to lower altitudes, the local LHR frequency increases. When the ray reaches a point where the LHR frequency equals the wave frequency, the refractive index curve becomes closed, making it possible for the wave normal to go through 90° and the ray direction to reverse. Whistlers that undergo such reflections in the magnetosphere are called magnetospherically reflected (MR) whistlers. Figure 7(b) illustrates MR reflection of a whistler at 1 kHz in a model magnetosphere. At a given frequency, there are usually a number of nonducted paths from a lightning source to a satellite, as illustrated in Fig. 10. A DE 1 satellite record of an MR whistler with multiple discrete components is shown in Fig. 2(b).

The effect of ions on whistler mode propagation leads to several other types of whistlers which have been named according to their propagation characteristics: pararesonance whistler (PR), paralongitudinal whistler (PL), transverse whistler, subprotonospheric whistler, and ion-cyclotron whistler. These are summarized by Park (4).

WHISTLER–LIGHTNING CORRELATIONS

Most of the whistler research in the last ~40 years has been conducted in the absence of detailed information about the location, intensity, and other parameters of the associated lightning sources. Recently, simultaneous lightning data as recorded by the National Lightning Network and whistler data as recorded on the ground stations in Antarctica and DE 1 satellite have become available (22,23). These data have made it possible to quantitatively assess the contributions to magnetospheric wave levels from individual discharges and localized storm centers. The general conclusions of these works are: (1) lightning can excite ducted whistler paths whose ionospheric endpoints are at ranges up to 2500 km or more from the lightning location, (2) a roughly linear relationship was found between two hop ducted whistler amplitudes in a few kilohertz range and range-normalized lightning field data in a similar frequency interval, (3) about 50% to 65% of the electromagnetic energy from individual lightning discharges injected into the ionosphere as far as 4500 km from the discharge can be detected as a nonducted whistler in the magnetosphere, (4) direct whistler and the first MR component intensities increase with increase in the causative lightning discharge current, (5) about one to two times as many whistlers are recorded by DE 1 as the number of C-G lightning strokes recorded by the lightning network, indicating the predominant role played by the intracloud and intercloud lightning in determining the wave levels in the magnetosphere.

EFFECTS OF WHISTLERS ON THE GEOSPACE ENVIRONMENT

The whistlers have important effects on Earth's near neutral atmosphere, ionosphere, and the magnetosphere up to about ~50,000 km where whistlers are observed. They pose a radio interference in the VLF range which is used for marine navigation and communication on the ground. They play an active role in the dynamics of the Earth's ionosphere and the magnetosphere through their interactions with the plasma and radiation belt energetic particles.

Spherics and Whistlers as a Source of VLF Radio Noise

The dominant natural radio noise below 30 MHz is atmospheric noise (spherics) from lightning discharges produced during thunderstorms. This noise has a moderately broad spectrum with large amplitude between 2 kHz and 30 kHz (24,25). At any receiving location, spherics can be received from the entire Earth's surface (at VLF frequencies). Therefore, the satisfactory design of a radio communication system must take into account the level and other characteristics of this atmospheric noise. It is estimated that only a small fraction, perhaps 1% or less, of the lightning discharges produce detectable whistlers (4). Thus, whistlers contribute only a small fraction of radio noise in the 2 kHz to 30 kHz band. Spaulding (24) has discussed the effects of atmospheric noise on telecommunication system performance.

Wave-Particle Interactions and Energetic Particle Effects

The magnetosphere contains energetic electrons and ions trapped in the Earth's magnetic field. The trapped energetic particles form the inner and outer radiation belts in the magnetosphere. The energetic particles comprise only a small fraction of the total particle population, most of which consists of *cold* electrons and ions; therefore, the cold plasma approximation is justified if we limit ourselves to the analysis of propagation velocity. However, the amplitude of whistlers may be strongly affected by energetic particles through resonant interactions that allow the conversion of particle energy to wave energy and vice versa.

Resonant conversion of kinetic energy of particles to wave energy or vice versa can take place by two different mechanisms depending on whether the particle motion along the geomagnetic field (longitudinal motion) or the particle motion transverse to the magnetic field is the controlling factor. The former mechanism, called Landau resonance, leads to flow or beam instabilities (or damping) and the latter to gyroresonance (or cyclotron resonance) instabilities (or damping). A general resonance condition for a plasma consisting of ions and electrons is given by:

$$f - \frac{1}{2\pi}k_{\parallel}v_{\parallel} + nf_{Hi} = 0, \quad n = 0, \pm1, \pm2\ldots \tag{28}$$

where, $k_{\parallel}$ and $v_{\parallel}$ are, respectively, the components of the wave normal vector $\boldsymbol{k}$ and particle velocity $\boldsymbol{v}$ along the geomagnetic field, and $f_{Hi} = |(q_iB)/(2\pi m_i)|$ is the gyrofrequency of a plasma particle with charge q_i and mass m_i. The wave frequency f is not an independent variable but is a unique function of $\boldsymbol{k}$. For any given mode this relation is given by the dispersion relation (3.3). For $n = 0$ in Eq. (28) we obtain the Landau resonance condition for beam instabilities where the parallel wave phase velocity equals the particle parallel velocity. All other values of n represent gyroresonances (or nth order gyroresonances), in which the wave frequency in the frame of reference of a particle equals some harmonic of the particle's gyrofrequency. The principal gyroresonance, given by $n = -1$, occurs for a wave frequency in the counter streaming particle's frame of reference equal to its gyrofrequency. Under gyroresonance, electrons and ions produce waves near their respective gyrofrequencies. For lightning-generated whistlers, the strongest resonant interaction takes place with radiation belt electrons in the 1 keV to >200 keV range which have their gyrofrequency in the VLF range.

Whistler Amplification and Emission Triggering. A large fraction of ducted whistlers show evidence of amplification in the magnetosphere. Amplification usually occurs in a limited frequency range that depends on the parameters of energetic electron population in the magnetosphere. Amplified whistlers frequently trigger free-running emissions, as illustrated in Fig. 2(a). There is a strong preference for triggering at the half-minimum gyrofrequency, but occasionally an emission might be triggered by the low-frequency tail of a whistler (11). Several dozen high power transmitters operate around the world in the ~10 kHz to 30 kHz frequency range for purposes of communication and navigation. Signals from these transmitters enter the magnetosphere and propagate in the whistler mode. These transmitter signals, when received at a ground station in the conjugate hemisphere, show evidence of

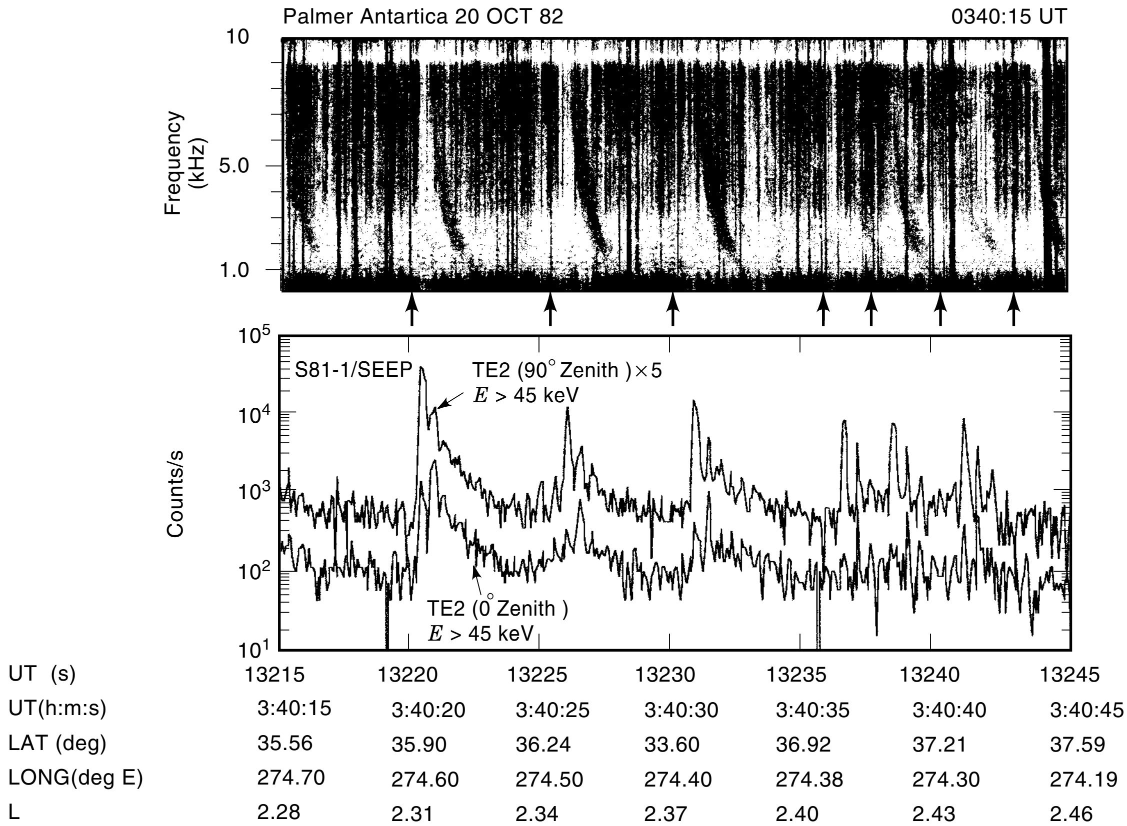

Figure 11. Examples of LEP events observed on the low altitude SEEP satellite and correlated whistler observations at Palmer (L = 2.4, 64°W), Antarctica. (From W. L. Imhof et al., *J. Geophys. Res.,* **94**: 10079, 1989. Copyrighted by the American Geophysical Union. With permission.)

wave amplification and emission triggering. An experimental transmitter facility capable of radiating up to a few kilowatts in the ~2 kHz to 5 kHz range was operated at Siple Station, Antarctica, between 1973 and 1988 to study the physics of wave-particle interactions. The waves injected into the magnetosphere from Siple Station were received at the magnetically conjugate points at Roberval and Lake Mistissini in Canada. Amplitude measurements of received signals show that they are typically amplified by ~30 dB during one passage through the magnetosphere. Siple transmitter experiments have also revealed many highly dynamic and nonlinear wave-particle and wave-wave interaction effects (4,6).

Energetic Electron Precipitation. Wave-particle interactions that amplify whistlers and trigger emissions also result in the perturbation of energetic electron orbits such that some of the interacting electrons precipitate into the upper atmosphere. Precipitating electrons produce optical emissions, Bremstrahlung X rays, and enhanced ionization in the ionosphere (26–28). Experimental evidence indicates that ducted whistlers, propagating essentially along the magnetic field lines, regularly precipitate energetic electrons producing ionospheric disturbances consistent with precipitation of 10^2 to 10^4 el $\cdot$ cm$^{-2}\cdot$ sr$^{-1}\cdot$ s^{-1} of >100 keV electrons (29). The Stimulated emission of energetic particles (SEEP) experiment on the low-altitude S81-1 spacecraft provided the first direct evidence of the removal of the electrons from the radiation belts by whistlers (30). These events, called lightning-induced electron precipitation (LEP), regularly occur throughout the plasmasphere and are important on a global scale as a loss process for the radiation belt electrons (31). Figure 11 shows examples of LEP events.

Most of the lightning energy injected into the magnetosphere propagates as nonducted whistlers. These obliquely propagating whistlers reflect between the hemispheres, often persisting for many tens of seconds [see Fig. 2(b)]. They can interact strongly with relatively low energy (10 eV to 10 keV) electrons, precipitating significant fluxes of superthermal (e.g., 100 eV) electrons, producing ionization enhancements at 200 km to 300 km and leading to the formation of whistler-mode ducts (32).

Ionospheric Density Perturbations and Their Effects on Transmitter Signals. Since 1963, certain transient perturbations of subionospheric VLF, low frequency (LF), and medium frequency (MF) signals, sometimes called Trimpi events (named after their discoverer), have been known to occur in association with ground-based observations of whistlers. These perturbations of signal amplitude and phase, characterized by a sudden onset of about 0.5 s to 1.5 s duration and a roughly exponential recovery lasting about 1 min, are attributed to secondary ionization in the lower ionosphere (D and E regions) caused by whistler-associated electron precipitation discussed previously (27). In recent years the perturbations in VLF transmitter signals have been used as a sensitive technique for detecting particle precipitation (28).

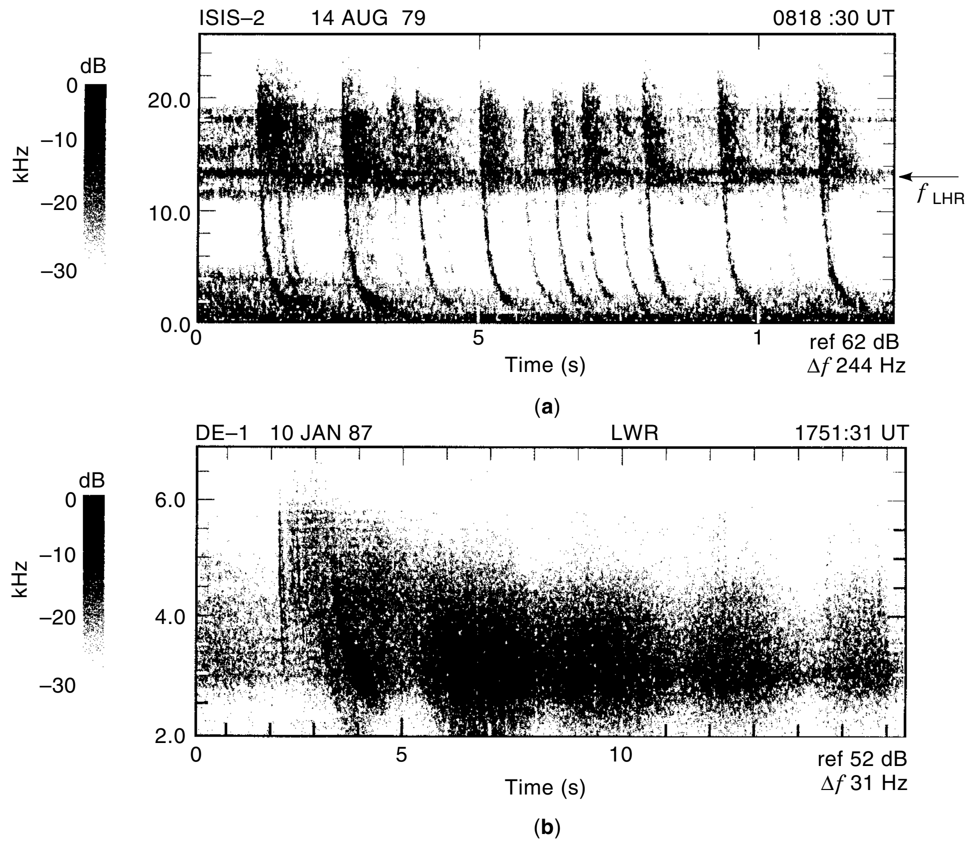

Figure 12. (a) ISIS-2 satellite observations of lower hybrid waves near 10 kHz excited by whistlers. (b) DE 1 satellite observations of hiss band excited by whistler. (Courtesy of VLF group, Stanford University.)

Generation of Lower Hybrid Resonance Emissions and Plasmaspheric Hiss

Whistlers generate strong lower hybrid waves throughout large regions of the topside ionosphere and magnetosphere (18,33). Figure 12(a) shows whistler-excited lower hybrid waves observed on the ISIS-2 satellite. Recent work by Bell and Ngo (33) suggests that LH waves are excited by a passive linear mode coupling as the nonducted whistlers are scattered by small scale (~1 m) field-aligned plasma density irregularities. The necessary excitation conditions can be readily satisfied at midlatitude and high latitude at altitudes up to two earth radii. In the topside ionosphere directly over thunderstorm cells, the intense whistlers from lightning discharges excite LHR waves with broadband intensities of 100 mV/m or more. These LHR waves can interact with suprathermal H^+ ions with energy ≥6 eV and heat them by 20 eV to 40 eV (34).

Data from the DE 1 satellite show that whistlers can often trigger hiss emissions that endure for up to 10 s to 20 s periods. Figure 12(b) shows an example of whistler-triggered hiss emission. Plasmaspheric hiss is a steady incoherent noise observed throughout the plasmasphere and is believed to be the dominant contributor to the loss of radiation belt particles. However, the mechanism for generation and sustenance of hiss are not yet understood. It has been suggested that whistlers may contribute to the generation and sustenance of hiss (35,36).

CONCLUDING REMARKS

Great advances have been made in our understanding of whistler in the last 45 years since Storey first explained the phenomenon in 1953. Whistlers are important partly because they have proven to be a valuable remote sensing tool in our investigations of the upper atmosphere, and partly because they influence the behavior of the ionosphere and the magnetosphere.

We conclude by pointing out the potentially important role that lightning and lightning-generated whistlers may be playing in the physics of magnetospheric plasma waves and particles. It has been widely assumed that most of the plasma waves are generated from background noise levels within the magnetosphere via wave particle interactions with energetic particles supplying the free energy (37). Recent results show that lightning can be an important source of (1) plasmaspheric hiss believed to be responsible for the slot region in the radiation belts (35,36), (2) lower hybrid waves that can heat and accelerate protons to suprathermal temperatures (34), and (3) ULF magnetic fields that can influence the generation and amplification of geomagnetic pulsations (38). Lightning-induced electron precipitation events (LEP) regularly occur throughout the plasmasphere and are important on a global scale as a loss process for the radiation belt electrons (28,31). Red sprites and blue jets are upper atmospheric optical phenomena associated with thunderstorms that have only recently been documented using low light-level television technology. Intense efforts, both experimental and theoretical, are presently underway to ascertain whether these phenomena may create locally or globally significant long lived electrochemical residues within the upper atmosphere (39,40). Approximately 2000 thunderstorms are active near the Earth's surface at any given time, and on the average, lightning strikes the Earth ~100 times/s (41). The average lightning discharge radiates an intense pulse of ~20 Gigawatts peak power which propagates through the lower atmosphere and into the ionospheric and magnetospheric plasmas, generating new waves, heating, accelerating, and precipitating components of the charged particles comprising these plasmas. Thus, future investigations should consider electromagnetic energy released in the thunderstorms as an important free energy source for the generation of magnetospheric plasma waves and for maintaining radiation belt equilibrium via wave-particle interactions and particle precipitation.

BIBLIOGRAPHY

1. H. Barkhausen, Zwei mit Hilfe der neuen Verstarker entdeckte Erscheinungen, *Physik. Z.,* **20** (1919): 401, 1919.
2. L. R. O. Storey, An investigation of whistling atmospherics, *Philos. Trans. R. Soc. London, Ser. A.,* **246**: 113, 1953.
3. R. A. Helliwell, *Whistlers and Related Ionospheric Phenomena,* Stanford: Stanford Univ. Press, 1965.
4. C. G. Park, Whistlers, in V. Volland (ed.), *Handbook of Atmospherics,* vol. 2, Boca Raton, FL: CRC Press, 1982, pp. 21–77.
5. M. Hayakawa, Whistlers, in V. Volland (ed.), *Handbook of Atmospheric Electrodynamics,* vol. 2, Boca Raton, FL: CRC Press, pp. 156–193.
6. V. S. Sonwalkar, Magnetospheric LF-, VLF-, and ELF-waves, Chapter II/13, *Handbook of Atmospheric Electrodynamics,* Boca Raton, FL: CRC Press, 1995.
7. K. G. Budden, *The Propagation of Radio Waves,* Cambridge, UK: Cambridge Univ. Press, 1985.
8. T. H. Stix, *Waves in plasmas,* New York: American Inst. Physics, 1992.
9. R. L. Smith, Propagation characteristics of whistlers trapped in field-aligned columns of enhanced ionization, *J. Geophys. Res.,* **66** (11): 3699, 1961.
10. R. L. Smith and J. J. Angerami, Magnetospheric properties deduced from OGO 1 observations of ducted and non-ducted whistlers, *J. Geophys. Res.,* **73** (1): 1, 1968.
11. D. L. Carpenter, Ducted whistler mode propagation in the magnetosphere: A half-gyrofrequency upper intensity cutoff and some associated wave growth phenomena, *J. Geophys. Res.,* **73**: 2919, 1968.
12. U. S. Inan and T. F. Bell, The plasmapause as a VLF wave guide, *J. Geophys. Res.,* **82** (19): 2819, 1977.
13. J. J. Angerami, Whistler duct properties deduced from VLF observations made with the OGO-3 satellite near the magnetic equator, *J. Geophys. Res.,* **75** (31): 6115, 1970.
14. V. S. Sonwalker et al., Simultaneous observations of VLF ground transmitter signals on the DE 1 and COSMOS 1809 satellites: Detection of a magnetospheric caustic and a duct, *J. Geophys. Res.,* **99** (17): 511, 1994.
15. R. A. Helliwell et al., The "nose" whistler-a new high latitude phenomenon, *J. Geophys. Res.,* **61** (1): 20, 139–142, 1956.
16. D. L. Carpenter and N. Seely, Cross-L plasma drifts in the outer plasmasphere: Quiet time patterns and some storm related effects, *J. Geophys. Res.,* **81**: 2728, 1976.
17. S. S. Sazhin, M. Hayakawa, and K. Bullough, Whistler diagnostics of magnetospheric parameters: A review, *Ann. Geophys.,* **10**: 293, 1992.
18. N. M. Brice and R. L. Smith, Lower hybrid resonance emissions, *J. Geophys. Res.,* **70**: 71, 1965.
19. W. J. Burtis, Electron concentration calculated from the lower hybrid resonance band observed by OGO-3, *J. Geophys. Res.,* **78**: 5515, 1973.
20. R. E. Barrington, J. S. Belrose, and G. L. Nelms, Ion composition and temperature at 1000 km as deduced from the simultaneous observations of a VLF plasma resonance and topside sounder data from Alouette I satellite, *J. Geophys. Res.,* **70**: 1647, 1965.
21. I. Kimura, Effects of ions on whistler-mode raytracing, *Radio Sci.,* **1**: 269, 1966.
22. D. L. Carpenter and R. E. Orville, The excitation of active whistler mode signal paths in the magnetosphere by lightning: Two case studies, *J. Geophys. Res.,* **94**: 8886, 1989.
23. V. S. Sonwalkar et al., Thunderstorm Coupling to the Magnetosphere: (1) Whistler-lightning correlations, (2) Contribution of lightning energy to the magnetosphere, (3) Lightning as a source of hiss, *Proc. 25th General Assembly Int. Union Radio Sci.,* **H1-7** (444): 28 Aug.–5 Sept. 1996, Lille, France, 1996.
24. A. D. Spaulding, Atmospheric noise and its effects on telecommunication system performance, Chapter I/14, *Handbook of Atmospheric Electrodynamics,* Boca Raton, FL: CRC Press, April, 1995.
25. J. L. Norman Violette, D. R. J. White, and M. F. Violette, *Electromagnetic Compatibility Handbook,* New York: Von Nostrand Reinhold, 1987.
26. R. A. Helliwell et al., Correlations between λ4278 optical emissions and VLF wave events observed at $L \simeq 4$ in the Antarctic, *J. Geophys. Res.,* **85**: 3376, 1980.
27. R. A. Helliwell, J. P. Katsufrakis, and M. L. Trimpi, Whistler-induced amplitude perturbation in VLF propagation, *J. Geophys. Res.,* **78**: 4679, 1973.
28. U. S. Inan et al., Subionospheric VLF signatures of nighttime D-region perturbations in the vicinity of lightning discharges, *J. Geophys. Res.,* **93**: 11455, 1988.
29. W. C. Burgess and U. S. Inan, Simultaneous disturbance of conjugate ionospheric regions in association with individual lightning flashes, *Geophys. Res. Lett.,* **17** (3): 259–262, 1990.
30. H. D. Voss et al., Lightning induced electron precipitation, *Nature,* **312**: 740, 1984.
31. W. C. Burgess and U. S. Inan, The role of ducted whistlers in the precipitation loss and equilibrium flux of radiation belt electrons, *J. Geophys. Res.,* **98** (A9): 15643, 1993.
32. D. Jasna, U. S. Inan, and T. F. Bell, Precipitation of suprathermal (100 EV) electrons by oblique whistler waves, *Geophys. Res. Lett.,* **19**: 1639–1642, 1992.
33. T. F. Bell and H. D. Ngo, Electrostatic lower hybrid waves excited by electromagnetic whistler mode waves scattering from planar magnetic-field-aligned plasma density irregularities, *J. Geophys. Res.,* **95**: 149, 1990.
34. T. F. Bell et al., The heating of suprathermal ions above thunderstorm cells, *Geophys. Res. Lett.,* **20**: 1991–1994, 1993.
35. V. S. Sonwalkar and U. S. Inan, Lightning as an embryonic source of VLF hiss, *J. Geophys. Res.,* **94**: 6986, 1989.
36. A. B. Draganov et al., Whistlers and plasmaspheric hiss: Wave directions and three-dimensional propagation, *J. Geophys. Res.,* **98** (A7): 11401–11410, 1993.
37. L. R. Lyons and D. J. Williams, *Quantitative Aspects of Magnetosphere Physics,* Norwell, MA: Kluwer, 1984.
38. A. C. Fraser-Smith, ULF magnetic fields generated by electrical storms and their significance to geomagnetic pulsation generation, *Geophys. Res. Lett.,* **20**: 467, 1993.
39. D. D. Sentman et al., Preliminary results from the Sprites94 Aircraft Campaign: 1. Red Sprites, *Geophys. Res. Letts.,* **22**: 1205–1208, 1995.
40. E. M. Wescott et al., Preliminary results from the Sprites94 Aircraft Campaign: 2. Blue Jets, *Geophys. Res. Letts.,* **22**: 1209–1213, 1995.
41. H. Volland, *Atmospheric Electrodynamics,* New York: Springer-Verlag, 1984.

VIKAS S. SONWALKAR
University of Alaska Fairbanks